

Scalar-induced gravitational wave from domain wall perturbation

Bo-Qiang Lu^{a,1}

^aSchool of Science, Huzhou University, Huzhou, Zhejiang 313000, China

E-mail: bqlu@zjhu.edu.cn

ABSTRACT: Domain walls represent two-dimensional topological defects that emerge from the spontaneous breaking of discrete symmetries in various new physics models. In this study, we undertake the first calculation of gravitational waves produced by scalar perturbations generated from the domain wall network. Our findings indicate that the gravitational wave spectrum is notably distinct from that of other sources. This opens up a promising avenue for future gravitational wave experiments aimed at exploring the role of domain walls in the early Universe. Our results could significantly enhance the capabilities of gravitational wave experiments, serving as a valuable method for testing new physics and better identifying diverse sources of gravitational waves.

Contents

1	Introduction	2
2	Perturbations from domain wall	4
2.1	The curvature perturbation by domain wall	4
2.2	The power spectrum of the curvature perturbation	6
3	Induced gravitational wave	7
3.1	The tensor mode of the induced GW	7
3.2	Gravitational wave power spectrum	9
4	Gravitational wave from perturbation of domain wall	12
4.1	Spectrum before domain wall annihilation	12
4.2	Spectrum after domain wall annihilation	12
4.3	Results	17
5	Conclusions	18
A	Domain wall evolution	19

1 Introduction

The detections of the gravitational waves (GWs) from mergers of binary black holes since 2015 by LIGO have opened an era of GW astronomy [1]. Recent observations from pulsar timing arrays (PTAs) further indicate the existence of a stochastic GW background at nano-Hz band [2–5]. Thanks to the weak interactions between GW and matter, once the GWs are produced in the early Universe, they can propagate freely without absorption or scattering by the plasma. Therefore, the GWs can be an ideal probe of the Universe before Big Bang Nucleosynthesis (BBN). There may exist plenty of GW sources in the early Universe, including the first-order phase transition, quantum fluctuations during inflation, oscillations of the cosmic string, and the annihilation of the domain walls (DWs) (see Ref. [6] for a review).

The scalar-induced GW is a general mechanism for the production of the GW, in which the curvature perturbations source the tensor perturbations at second order, although the scalar and tensor modes are linearly independent at first order in the perturbation cosmology (see Ref. [7] for a recent review on this topic). In previous literature, the (re-)entry of the super-horizon mode of the scalar perturbation produced during cosmic inflation is commonly considered as a primary source for the scalar-induced GW. The observations at the cosmic microwave background (CMB) scale have restricted the nearly scale-invariant primordial power

spectrum of scalar perturbations to be of order $\sim 10^{-9}$. One might then expect that the GW power spectrum at second order has a magnitude $\sim 10^{-18}$ and is too small to be probed by the GW experiments [8]. Generally, the power spectrum of the scalar perturbation can be scale-dependent, for instance, the multi-scalar inflation models [8–10]. Furthermore, the density perturbations can grow if the early Universe undergoes a period dominated by dust, for example, the primordial black holes (PBHs) [11–16]. The perturbations from PBH density fluctuation are initially isocurvature perturbations in the radiation-dominated Universe and later become curvature perturbations deep in the dust-dominated Universe [16]. In these situations, the second-order GW could be enhanced at small scales and can be comparable to that of the first-order [14]. In this work, we will calculate the curvature perturbations generated by the DW network and the second-order GWs induced by such perturbations. Since the fraction of total energy density in DWs grows with time, the amplitudes of the perturbation from DW are proportional to the scale, which might lead to a significant production of GWs at large scales (note that the ‘large scale’ mentioned here is much smaller than the CMB scale) before the annihilation of the wall.

The DW is a sheet-like topological defect generated during the spontaneous breaking of a discrete symmetry. In the scaling regime, the DW energy density is estimated as $\rho_w = \mathcal{A}\sigma_w/t$, where σ_w is the surface tension of the wall, while the energy density of the radiation is $\rho_{\text{rad}} = 3/(32\pi Gt^2)$. After a time $t \sim 1/(G\sigma_w)$, the DW energy density would dominate the Universe, leading to the so-called DW problem. Introducing a discrete symmetry-breaking operator to generate a bias potential is a common solution to the DW problem. DWs begin annihilation once the bias potential becomes comparable with the energy density of the wall. If DWs existed for a while and their energy density accounts for about 10% of the total energy density, the evolution of DW could lead to observable cosmological phenomena. It has been shown that the annihilation of the DW generated at a scale $\simeq 200$ TeV due to the QCD instanton-induced bias potential during the QCD phase transition can naturally explain the recent PTAs observations [17, 18], such as NANOGrav 15-year dataset [2] and IPTA-DR2 dataset [19]. Recently, the author has shown in Refs. [20, 21] that the Poisson fluctuations in the DW network could lead to horizon-sized overdense regions whose collapse could form PBHs. This mechanism for the production of PBH can be significant when the energy fraction of the DW is ~ 0.1 . A lesson from this result is that the induced GW from the scalar perturbations by DW might also be remarkable [22, 23]. In this work, we will present the calculations of the scalar-induced GW spectrum from DW’s perturbation in detail. In the upcoming work, we will provide the detection prospect for these induced GW signals in future space-based GW experiments.

This work is arranged as follows. In section 2, we calculate the curvature perturbation generated by the DW. In section 3, we provide the general formulas for the GW induced by the scalar perturbation in the second order. Then, we calculate the induced GW spectrum from the DW perturbation in section 4. Finally, we summarize our results and conclusions in section 5. In appendix A, we provide the formulas for the evolution of the correlation length of DW.

2 Perturbations from domain wall

In this section, we first calculate the first-order scalar perturbations in the metric by the DW. Then, we determine the power spectrum of the curvature perturbations for the induced GW.

2.1 The curvature perturbation by domain wall

Consider the linearly-perturbed Friedmann-Lemaitre-Robertson-Walker metric with a second-order tensor perturbation h_{ij} in the Newtonian gauge for a spatially flat universe

$$ds^2 = a^2(\eta) \left\{ -(1 + 2\Psi)d\eta^2 + \left[(1 + 2\Phi)\delta_{ij} + \frac{h_{ij}}{2} \right] dx^i dx^j \right\}, \quad (2.1)$$

where the conformal time η is related to the cosmic time by $dt = a d\eta$, the Newtonian potential Ψ and intrinsic curvature perturbation Φ are gauge-invariant quantities, which are combinations of metric perturbations, h_{ij} is the second-order tensor mode with $h_i^i = 0$. We neglect the first-order tensor mode and the vector perturbations. In the radiation era, the scale factor, Hubble rate, and energy density evolve as $a(\eta) = a_i \eta / \eta_i$, $\mathcal{H} = aH = \eta^{-1}$, and $\rho_{\text{rad}} \propto \eta^{-4}$. We note that the perturbation theory at second order suffers from the so-called gauge issue: the theory is not gauge invariant under the gauge transformation, therefore, the derived tensor spectrum depends on the choice of the gauge (see Ref. [7] for a review). A coincidence was found previously that in a radiation-dominated Universe, the numerical results for the induced tensor spectrum in the Newtonian gauge and in the synchronous gauge are shown to be the same [24–26].

Let us first consider a universe filled with pure static DWs. The gauge-invariant scalar perturbations obey the linearized Einstein equations given by [27, 28]

$$\nabla^2 \tilde{\Phi} = -4\pi G a^2 \bar{\rho} \Delta, \quad (2.2)$$

$$\nabla^2 (\tilde{\Phi} + \tilde{\Psi}) = 8\pi G a^2 \bar{p} \Pi, \quad (2.3)$$

where $\bar{\rho}$ and \bar{p} denote the background values of the energy density and pressure, respectively. Δ is the relative energy density perturbation and Π is the anisotropic stress. We use the tilde to denote the corresponding values of the scalar perturbations in the universe purely filled with DWs. Given a thin DW (neglecting the thickness of the wall) located in xy -plane at position $x = 0$ (in this section, we use x , y , and z to denote the co-moving coordinate), the energy-momentum tensor of the wall in the wall frame is given by [27]

$$T_{\mu\nu} = \sigma_w \delta(ax) \text{diag}(1, 0, -1, -1), \quad (2.4)$$

where σ_w is the surface tension of the wall and $\delta(x)$ is the Dirac-delta function whose dimension is $1/x$. Therefore, the anisotropic press of the wall is $\bar{p}\Pi = -\sigma_w \delta(ax)$. Then the linearized Einstein equations (2.2) and (2.3) for the DW become

$$\nabla^2 \tilde{\Phi}(x) = -4\pi G a^2 \sigma_w \delta(ax) \quad (2.5)$$

$$\nabla^2 [\tilde{\Psi}(x) + \tilde{\Phi}(x)] = -8\pi G a^2 \sigma_w \delta(ax) \quad (2.6)$$

We observe from Eq. (2.5) and (2.6) that unlike the non-relativistic matter which has an attractive gravity, the gravitational force of the wall is repulsive [27]. Together with Eq. (2.6), we observe $\tilde{\Psi}(x) = \tilde{\Phi}(x)$ for the DW.

Let us consider the solution for the scalar potential $\tilde{\Psi}$. From Eq. (2.5) we know that at the position $x = 0$, the potential is continuous while its derivative has a jump discontinuity, therefore, the solution must be a function of $|x|$. By requiring $\tilde{\Psi}(x) = \tilde{\Psi}(-x)$ and $\tilde{\Psi}(x) \propto 1/|x|$ at large distance, the solution for Eq. (2.5) is [28]

$$\tilde{\Psi}(x) = 2\pi G a(\eta) \sigma_w (\sqrt{x^2 + d_w^2} - |x|), \quad (2.7)$$

where d_w is the separation length of the wall in the co-moving coordinate and is related to the physical correlation length L_w by $d_w = L_w/a(\eta)$. Suppose there are a set of walls located at positions $x_j = j d_w$ with $j = 0, \pm 1, \pm 2, \dots$, we can then approximate the potential (2.7) by a cosine function, i.e.,

$$\tilde{\Psi}(x) = 2\pi G a(\eta) \sigma_w \sum_j (\sqrt{(x - j d_w)^2 + d_w^2} - |x - j d_w|) \simeq C \cos^2(\pi x/d_w) \quad (2.8)$$

where the coefficient C is determined by the condition that the averaged value within a separation distance of both potentials are equal to each other, we then have $C \simeq \pi G \sigma_w L_w$. The Fourier components of the potential is then given by

$$\tilde{\Psi}_k(\eta) = \frac{C}{2} \sqrt{\frac{\pi}{2}} \delta\left(k - \frac{2\pi}{d_w}\right), \quad (2.9)$$

where k is the co-moving wave number which is related to the physical frequency by $k = a f$ so that one has $k d_w = f L_w$ (we assume the scale of the Universe at present is $a(\eta_0) = 1$, where $\eta_0 = 1.47 \times 10^{18}$ s is the conformal time today).

In this work, we will consider a radiation-dominated Universe, in which the DWs are generated via the spontaneous breaking of a discrete symmetry. We require that the DWs be annihilated by a biased potential before they dominate the Universe. In the following, Φ and Ψ are used to denote the values of the perturbations in the two-component Universe. Then the anisotropic stress for the two-component Universe is $\Pi = f_\gamma \Pi_\gamma + f_w \Pi_w$, where $f_\gamma = \bar{\rho}_w/\bar{\rho}_{\text{tot}} \simeq 1$ and $f_w = \bar{\rho}_w/\bar{\rho}_{\text{tot}} \simeq \bar{\rho}_w/\bar{\rho}_{\text{rad}}$ are the energy density fraction of the radiation and DW, respectively. Π_γ and Π_w are the anisotropic pressure from the radiation and wall, respectively. Since the radiation is a perfect fluid whose anisotropic stress is trivial, i.e., $\Pi_\gamma = 0$, the anisotropic stress for Eq. (2.3) in the two-component Universe is given by $\Pi = f_w(\eta) \Pi_w$. In the limit $f_w(\eta) \rightarrow 0$ (corresponding to the cases in which the DWs do not present or have decayed away), the anisotropic stress is absent and the linearized Einstein equations indicate $\Phi(x) = -\Psi(x)$. From the Einstein equations, we also know that $\tilde{\Phi}(x) = \tilde{\Psi}(x)$ in the DW-dominated universe, corresponding to the case $f_w(\eta) = 1$. Therefore, the curvature perturbation by DWs in a two-component Universe dominated by radiation can be estimated as

$$\Phi(\eta, x) \simeq f_w(\eta) \tilde{\Phi}(\eta, x) = f_w(\eta) \tilde{\Psi}(\eta, x). \quad (2.10)$$

It is worth mentioning that we do not apply this relation to the case with $f_w(\eta) = 0$, before the presence or after the annihilation of the DW.

2.2 The power spectrum of the curvature perturbation

We note that the potential, and therefore, the power spectrum obtained by Eq. (2.9) is one-dimensional (the definition of the power spectrum is given by Eq. (2.19)). Suppose isotropic perturbations, we can obtain the three-dimensional power spectrum $\Delta_{3\text{D}}(k)$ from the one-dimensional power spectrum $\Delta_{1\text{D}}(k)$ by [29]

$$\Delta_{3\text{D}}(k) = \frac{1}{k^2} \int_k^\infty \Delta_{1\text{D}}(y) y dy. \quad (2.11)$$

Using the one-dimensional potential (2.9) and Eq. (2.11) and considering the horizon-sized perturbation, we then obtain the three-dimensional isotropic power spectrum of the wall

$$\mathcal{P}_{\tilde{\Psi}}(k, \eta) = \frac{C^2 k^2}{16\pi} \delta\left(k - \frac{2\pi}{d_w}\right). \quad (2.12)$$

We therefore find that the three-dimensional potential in momentum space is obtained by the one-dimensional potential (2.9) with the replacement $\tilde{\Psi}_k(\eta) \rightarrow \tilde{\Psi}_k(\eta)/\sqrt{k}$. Combining the above results, the Fourier component of the curvature perturbation in the two-component Universe is given by

$$\Phi_k(\eta) = \frac{C f_w(\eta)}{2} \sqrt{\frac{\pi}{2k}} \delta\left(k - \frac{2\pi}{d_w}\right). \quad (2.13)$$

Eq. (2.13) indicates that the DW network is a continuous source of the curvature perturbation and the evolution of the power spectrum is encoded in the correlation length $L_w = a(\eta)d_w$ of the wall. We present the details for the evolution of L_w with cosmic time in appendix A. Following a rapid expansion, the DW enters into the scaling regime, in which L_w scales with the cosmic time as $L_w \simeq t/\mathcal{A}$, where $\mathcal{A} \simeq 1$ from the simulations [30]. The energy density of the wall is related to the correlation length via the one-scale assumption, i.e., $\rho_w = \sigma_w/L_w$. In the radiation dominated universe, the scale factor $a(\eta) = a_i\eta/\eta_i$, where η_i is the reference initial time. The cosmic time $dt = a(\eta)d\eta$ and we use the approximation $t \simeq a_i\eta^2/(2\eta_i)$. Then the correlation length is given by

$$L_w = \frac{a_i\eta^2}{2\mathcal{A}\eta_i} \quad \text{and} \quad d_w = \frac{L_w}{a(\eta)} = \frac{\eta}{2\mathcal{A}}. \quad (2.14)$$

The energy fraction of the wall is then given by

$$f_w(\eta) = \frac{\bar{\rho}_w}{\bar{\rho}_{\text{rad}}} = \frac{32}{3} \pi \mathcal{A} G \sigma_w t = \frac{32\pi \mathcal{A} G \sigma_w}{3} \frac{a_i\eta^2}{2\eta_i}. \quad (2.15)$$

Following the common practice in the literature, we decompose the potential as

$$\Phi_k(\eta) = T(x)\phi_k, \quad (2.16)$$

where ϕ_k denotes the value of the potential at the initial time η_i and $T(x)$ is a transfer function, which represents the changes in the amplitudes of the potential between η_i and η . In the following, we adopt the notation $x \equiv k\eta$. For our case, the two functions are given by

$$T(x) = x^5 \delta(x - 4\pi\mathcal{A}) \quad \text{and} \quad \phi_k = \frac{B}{k^5 \sqrt{k}}, \quad (2.17)$$

with

$$B = \frac{2^{\frac{3}{2}} \pi^{\frac{5}{2}} a_i^2 G^2 \sigma_w^2}{3\eta_i^2}. \quad (2.18)$$

Assuming Gaussian fluctuations, we can write the Bardeen potential as $\Phi_{\mathbf{k}}(\eta) = \Phi_{\mathbf{k}}(\eta) \hat{E}(\mathbf{k})$ [8], where \hat{E} is a Gaussian random variable of unit variance with the property $\langle \hat{E}^*(\mathbf{k}_1) \hat{E}(\mathbf{k}_2) \rangle = \delta^3(\mathbf{k}_1 - \mathbf{k}_2)$. The power spectrum for the scalar perturbation can then be defined as

$$\langle \Phi^*(\mathbf{k}_1) \Phi(\mathbf{k}_2) \rangle = \frac{2\pi^2}{k^3} \delta(\mathbf{k}_1 - \mathbf{k}_2) \mathcal{P}_{\Phi}(k, \eta). \quad (2.19)$$

Using the decomposition (2.16), the potential is given by $\Phi_{\mathbf{k}}(\eta) = T(k\eta) \phi_{\mathbf{k}}(k)$, with $\phi_{\mathbf{k}} = \phi_k \hat{E}(\mathbf{k})$ whose power spectrum is then given by

$$\mathcal{P}_{\phi}(k) = \frac{B^2}{2\pi^2 k^8}. \quad (2.20)$$

We observe that the power spectrum scales as k^{-8} , and therefore, becomes significant at a large scale. It is expected that the scalar-induced GW from DW perturbations can be significantly enhanced in the late stage.

3 Induced gravitational wave

The space correlations of the curvature perturbation serve as the source of the induced GW. In this section, we follow Refs. [8, 14, 31, 32] to calculate the gravitational wave induced by scalar perturbation at second-order.

3.1 The tensor mode of the induced GW

The evolution of the tensor mode is governed by [8]

$$h''_{ij} + 2\mathcal{H}h'_{ij} - \nabla^2 h_{ij} = -4\hat{T}_{ij}{}^{lm} \mathcal{S}_{lm}, \quad (3.1)$$

where the prime denotes a derivative to conformal time. The source term is given by

$$\mathcal{S}_{ij} = 4\Phi\Phi_{|ij} + 2\Phi_{|i}\Phi_{|j} - \frac{3}{8\pi G a^2 \rho} \left[\mathcal{H}^2 \Phi_{|i}\Phi_{|j} + 2\mathcal{H}\Phi_{|i}\Phi'_{|j} + \Phi'_{|i}\Phi'_{|j} \right], \quad (3.2)$$

where the pipe denotes the spatial covariant derivative [8]. Transfer to the Fourier space, Eq. (3.1) becomes

$$h_{\mathbf{k}}^{s''} + 2\mathcal{H}h_{\mathbf{k}}^{s'} + k^2 h_{\mathbf{k}}^s = 4S_{\mathbf{k}}^s, \quad (3.3)$$

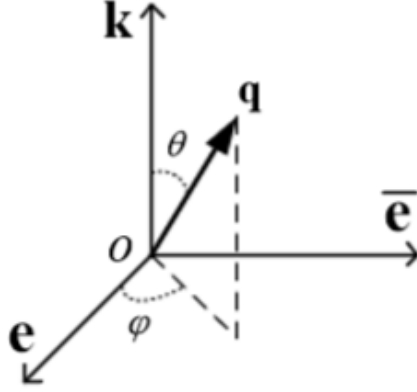


Figure 1: The momentum transfer \mathbf{q} in the coordinate system.

where $s = +, \times$ denotes the polarization mode of the GW, and the Fourier components of the tensor mode $h_{\mathbf{k}}^s$ are introduced by

$$h_{ij}(\eta, \mathbf{x}) = \int \frac{d^3\mathbf{k}}{(2\pi)^{3/2}} \left[h_{\mathbf{k}}^+(\eta) e_{ij}^+(\mathbf{k}) + h_{\mathbf{k}}^\times(\eta) e_{ij}^\times(\mathbf{k}) \right] e^{i\mathbf{k}\cdot\mathbf{x}}, \quad (3.4)$$

where the transverse traceless polarization tensors are defined as

$$e_{ij}^+(\mathbf{k}) = \frac{1}{\sqrt{2}} [e_i(\mathbf{k})e_j(\mathbf{k}) - \bar{e}_i(\mathbf{k})\bar{e}_j(\mathbf{k})], \quad (3.5)$$

$$e_{ij}^\times(\mathbf{k}) = \frac{1}{\sqrt{2}} [e_i(\mathbf{k})\bar{e}_j(\mathbf{k}) + \bar{e}_i(\mathbf{k})e_j(\mathbf{k})], \quad (3.6)$$

where $e(\mathbf{k})$ and $\bar{e}(\mathbf{k})$ are normalized vectors orthogonal to each other and to the GW propagation direction \mathbf{k} . The spatial coordinate system constructed by the vector set $\{e, \bar{e}, \mathbf{k}\}$ is depicted in Fig. 1. The source term $S_{\mathbf{k}}^s$ in the Fourier space is written as [14]

$$S_{\mathbf{k}}^s(\eta) = \int \frac{d^3\mathbf{q}}{(2\pi)^{3/2}} e_{ij}^s(\mathbf{k}) q_i q_j \left[2\Phi_{\mathbf{q}}\Phi_{\mathbf{k}-\mathbf{q}} + \frac{4}{3(1+w)} (\mathcal{H}^{-1}\Phi'_{\mathbf{q}} + \Phi_{\mathbf{q}}) (\mathcal{H}^{-1}\Phi'_{\mathbf{k}-\mathbf{q}} + \Phi_{\mathbf{k}-\mathbf{q}}) \right], \quad (3.7)$$

where $\omega = p/\rho$ is the equation of state parameter of the Universe. Using Eq. (2.16) for the potential $\Phi_{\mathbf{k}}$, the source can be written as [32]

$$S_{\mathbf{k}}^s(\eta) = \int \frac{d^3\mathbf{q}}{(2\pi)^{3/2}} e^s(\mathbf{k}, \mathbf{q}) F(\mathbf{q}, \mathbf{k} - \mathbf{q}, \eta) \phi_{\mathbf{q}} \phi_{\mathbf{k}-\mathbf{q}}, \quad (3.8)$$

where the symbols $e^s(\mathbf{k}, \mathbf{q}) \equiv e_{ij}^s(\mathbf{k}) q_i q_j$ and

$$F(\mathbf{q}, \mathbf{k} - \mathbf{q}, \eta) = 2T(q\eta)T(|\mathbf{k} - \mathbf{q}|\eta) + \frac{4}{3(1+w)} [\mathcal{H}^{-1}qT'(q\eta) + T(q\eta)] \times [\mathcal{H}^{-1}|\mathbf{k} - \mathbf{q}|T'(|\mathbf{k} - \mathbf{q}|\eta) + T(|\mathbf{k} - \mathbf{q}|\eta)]. \quad (3.9)$$

The solution to Eq. (3.3) can be obtained by the Green's function method

$$h_{\mathbf{k}}^s(\eta) = \frac{4}{a(\eta)} \int_{\eta_i}^{\eta} d\bar{\eta} G_{\mathbf{k}}(\eta, \bar{\eta}) a(\bar{\eta}) S_{\mathbf{k}}^s(\bar{\eta}), \quad (3.10)$$

where the Green's function $G_{\mathbf{k}}(\eta, \bar{\eta})$ is determined by solving

$$G_{\mathbf{k}}''(\eta, \bar{\eta}) + \left[k^2 - \frac{a''(\eta)}{a(\eta)} \right] G_{\mathbf{k}}(\eta, \bar{\eta}) = \delta(\eta - \bar{\eta}), \quad (3.11)$$

with the initial conditions

$$\lim_{\eta \rightarrow \bar{\eta}} G_{\mathbf{k}}(\eta, \bar{\eta}) = 0 \text{ and } \lim_{\eta \rightarrow \bar{\eta}} G_{\mathbf{k}}'(\eta, \bar{\eta}) = 1. \quad (3.12)$$

Using the relation $a(\eta) \propto \eta^{\frac{2}{1+3\omega}}$ for the scale factor, Eq. (3.11) can be written as

$$G_{\mathbf{k}}''(\eta, \bar{\eta}) + \left[k^2 - \frac{2(1-3\omega)}{1+3\omega} \eta^{-2} \right] G_{\mathbf{k}}(\eta, \bar{\eta}) = \delta(\eta - \bar{\eta}). \quad (3.13)$$

The general solution is found to be

$$kG_{\mathbf{k}}(\eta, \bar{\eta}) = \frac{\pi}{2} \sqrt{x\bar{x}} [Y_n(x)J_n(\bar{x}) - J_n(x)Y_n(\bar{x})], \quad (3.14)$$

where $J_n(x)$ and $Y_n(x)$ is the Bessel function of the first and second kind, with $n = \frac{1}{2} \sqrt{\frac{3(3-7\omega)}{1+3\omega}}$. For radiation-dominated Universe $\omega = 1/3$, the Green's function is given by

$$kG_{\mathbf{k}}(\eta, \bar{\eta}) = \sin(x - \bar{x}). \quad (3.15)$$

Eqs. (3.8)-(3.10) are the main results in this section, from which we can determine the tensor mode of the perturbations. The energy density of the tensor mode is given in the next subsection.

3.2 Gravitational wave power spectrum

The GWs can be distinguished from the background within a length-scale $\lambda \ll \ell \ll L_B$, where λ is the wavelength of GW and L_B is the typical length-scale of background [6]. In this scale, the GW energy density is given by

$$\rho_{\text{GW}}(\eta, \mathbf{x}) = \sum_{s=+, \times} \frac{M_{\text{Pl}}^2}{32a^2} \overline{\langle \nabla_i h_{\alpha\beta}^s \nabla^i h_{\alpha\beta}^s \rangle}, \quad (3.16)$$

where $M_{\text{Pl}} = 1/\sqrt{8\pi G}$ is the reduced Planck mass, i denotes the spatial components, the overline denotes the oscillation average over the length-scale ℓ and brackets represent an ensemble average. Using the Fourier expansion (3.4) of the GW we have

$$\rho_{\text{GW}}(\eta, \mathbf{x}) = \frac{M_{\text{Pl}}^2}{32a^2(2\pi)^3} \sum_{s=+, \times} \int d^3\mathbf{k}_1 \int d^3\mathbf{k}_2 k_1 k_2 \overline{\langle h_{\mathbf{k}_1}^s(\eta) h_{\mathbf{k}_2}^{s,*}(\eta) \rangle} e^{i(\mathbf{k}_1 - \mathbf{k}_2) \cdot \mathbf{x}}. \quad (3.17)$$

Let us first calculate the correlation function of the tensor in Eq. (3.17). Inserting the Green's function solution (3.10) for the GW, the correlation function is given by

$$\langle h_{\mathbf{k}_1}^{s_1}(\eta) h_{\mathbf{k}_2}^{s_2,*}(\eta) \rangle = \frac{16}{a^2(\eta)} \int_{\eta_i}^{\eta} d\bar{\eta}_1 G_{k_1}(\eta, \bar{\eta}_1) a(\bar{\eta}_1) \int_{\eta_i}^{\eta} d\bar{\eta}_2 G_{k_2}(\eta, \bar{\eta}_2) a(\bar{\eta}_2) \langle S_{\mathbf{k}_1}^{s_1}(\bar{\eta}_1) S_{\mathbf{k}_2}^{s_2,*}(\bar{\eta}_2) \rangle, \quad (3.18)$$

With the source term (3.8), we have

$$\begin{aligned} \langle S_{\mathbf{k}_1}^{s_1}(\bar{\eta}_1) S_{\mathbf{k}_2}^{s_2,*}(\bar{\eta}_2) \rangle &= \int \frac{d^3 \mathbf{q}_1}{(2\pi)^{3/2}} e^{s_1(\mathbf{k}_1, \mathbf{q}_1)} F(\mathbf{q}_1, \mathbf{k}_1 - \mathbf{q}_1, \bar{\eta}_1) \\ &\times \int \frac{d^3 \mathbf{q}_2}{(2\pi)^{3/2}} e^{s_2(\mathbf{k}_2, \mathbf{q}_2)} F^*(\mathbf{q}_2, \mathbf{k}_2 - \mathbf{q}_2, \bar{\eta}_2) \langle \phi_{\mathbf{q}_1} \phi_{\mathbf{k}_1 - \mathbf{q}_1} \phi_{\mathbf{q}_2}^* \phi_{\mathbf{k}_2 - \mathbf{q}_2}^* \rangle. \end{aligned} \quad (3.19)$$

Using the Wick theorem, the four-point correlation function can be decomposed as

$$\begin{aligned} \langle \Phi_{\mathbf{m}_1}(\bar{\eta}_1) \Phi_{\mathbf{m}_2}(\bar{\eta}_1) \Phi_{\mathbf{m}_3}^*(\bar{\eta}_2) \Phi_{\mathbf{m}_4}^*(\bar{\eta}_2) \rangle &= \langle \Phi_{\mathbf{m}_1}(\bar{\eta}_1) \Phi_{\mathbf{m}_2}(\bar{\eta}_1) \rangle \langle \Phi_{\mathbf{m}_3}^*(\bar{\eta}_2) \Phi_{\mathbf{m}_4}^*(\bar{\eta}_2) \rangle \\ &+ \langle \Phi_{\mathbf{m}_1}(\bar{\eta}_1) \Phi_{\mathbf{m}_3}^*(\bar{\eta}_2) \rangle \langle \Phi_{\mathbf{m}_2}(\bar{\eta}_1) \Phi_{\mathbf{m}_4}^*(\bar{\eta}_2) \rangle + \langle \Phi_{\mathbf{m}_1}(\bar{\eta}_1) \Phi_{\mathbf{m}_4}^*(\bar{\eta}_2) \rangle \langle \Phi_{\mathbf{m}_2}(\bar{\eta}_1) \Phi_{\mathbf{m}_3}^*(\bar{\eta}_2) \rangle \\ &= \delta(\mathbf{m}_1 - \mathbf{m}_2) \delta(\mathbf{m}_3 - \mathbf{m}_4) n_{\Phi}(\bar{\eta}_1) n_{\Phi}^*(\bar{\eta}_2) + 2 \langle \Phi_{\mathbf{m}_1}(\bar{\eta}_1) \Phi_{\mathbf{m}_3}^*(\bar{\eta}_2) \rangle \langle \Phi_{\mathbf{m}_2}(\bar{\eta}_1) \Phi_{\mathbf{m}_4}^*(\bar{\eta}_2) \rangle, \end{aligned} \quad (3.20)$$

where $\mathbf{m}_1 = \mathbf{q}_1$, $\mathbf{m}_2 = \mathbf{k}_1 - \mathbf{q}_1$, $\mathbf{m}_3 = \mathbf{q}_2$, and $\mathbf{m}_4 = \mathbf{k}_2 - \mathbf{q}_2$. Since the integration (3.19) does not change under a shift of the momentum transfer $\mathbf{q}_i \rightarrow \mathbf{k}_i - \mathbf{q}_i$ ($i = 1, 2$), the two terms in the second line of Eq. (3.20) equally contribute to the source correlator (3.19). Furthermore, the Dirac-delta functions in the first term in the third line of Eq. (3.20) give $\mathbf{q}_1 = \mathbf{k}_1/2$ and $\mathbf{q}_2 = \mathbf{k}_2/2$, which implies $\mathbf{q} \perp \mathbf{e}(\mathbf{k})$, $\bar{\mathbf{e}}(\mathbf{k})$, and therefore, $e^s(\mathbf{k}, \mathbf{q}) \equiv 0$ in this case. Thus, we find that the first term in the third line of Eq. (3.20) does not contribute to the source correlator (3.19).

Using the definition (2.19) for the power spectrum of the scalar perturbation, we have

$$\langle \phi_{\mathbf{m}_1} \phi_{\mathbf{m}_3}^* \rangle \langle \phi_{\mathbf{m}_2} \phi_{\mathbf{m}_4}^* \rangle = \delta(\mathbf{k}_1 - \mathbf{k}_2) \delta(\mathbf{q}_1 - \mathbf{q}_2) \left(\frac{2\pi^2}{q_1^3} \right) \left(\frac{2\pi^2}{(k_1 - q_1)^3} \right) \mathcal{P}(q_1) \mathcal{P}(k_1 - q_1). \quad (3.21)$$

In the following, we adopt the definitions $\mathbf{k}_1 = \mathbf{k}_2 \equiv \mathbf{k}$, $\mathbf{q}_1 = \mathbf{q}_2 \equiv \mathbf{q}$, $u = |\mathbf{k} - \mathbf{q}|/k$, and $v = q/k$. Then, Eq. (3.19) can be written as

$$\begin{aligned} \langle S_{\mathbf{k}_1}^{s_1}(\bar{\eta}_1) S_{\mathbf{k}_2}^{s_2,*}(\bar{\eta}_2) \rangle &= \frac{\pi}{2} \delta(\mathbf{k}_1 - \mathbf{k}_2) \int d^3 \mathbf{q} e^{s_1(\mathbf{k}, \mathbf{q})} e^{s_2(\mathbf{k}, \mathbf{q})} \\ &\times F_k(u, v, \bar{\eta}_1) F_k^*(u, v, \bar{\eta}_2) \frac{\mathcal{P}_{\phi}(q) \mathcal{P}_{\phi}(|\mathbf{k} - \mathbf{q}|)}{q^3 |\mathbf{k} - \mathbf{q}|^3}, \end{aligned} \quad (3.22)$$

where $F_k(u, v, \eta) \equiv F(\mathbf{q}, |\mathbf{k} - \mathbf{q}|, \eta)$. With the relations $q = vk$ and $\cos \theta = [k^2 + q^2 - (uk)^2]/(2kq) = (1 + v^2 - u^2)/(2v)$, we can convert the integration variables from (q, θ, φ) to (v, u, φ) , i.e.,

$$\int d^3 \mathbf{q} = \int_0^{\infty} q^2 dq \int_{-1}^1 d(-\cos \theta) \int_0^{2\pi} d\varphi = 2k^3 \int_0^{\infty} v dv \int_{|1-v|}^{1+v} u du \int_0^{2\pi} d\varphi. \quad (3.23)$$

Note that the functions $F(u, v, \eta)$ and $\mathcal{P}_\phi(k)$ are φ -independent, therefore, we can directly integrate out the variable φ in Eq. (3.22). From Fig. 1 we have the relations $e(\mathbf{k}) \cdot \mathbf{q} = q \sin \theta \cos \varphi$, $\bar{e}(\mathbf{k}) \cdot \mathbf{q} = q \sin \theta \sin \varphi$, and $e_{ij}^{s_1} e_{ij}^{s_2} = \delta^{s_1 s_2}$. Then the integration over φ is given by

$$\int_0^{2\pi} e^{s_1}(\mathbf{k}, \mathbf{q}) e^{s_2}(\mathbf{k}, \mathbf{q}) d\varphi = \begin{cases} \frac{\pi k^4}{32} [4v^2 - (1 - u^2 + v^2)^2]^2, & \text{for } s_1 = s_2, \\ 0, & \text{for } s_1 \neq s_2. \end{cases} \quad (3.24)$$

With these results, Eq. (3.22) can be written as

$$\begin{aligned} \langle S_{\mathbf{k}_1}^{s_1}(\bar{\eta}_1) S_{\mathbf{k}_2}^{s_2,*}(\bar{\eta}_2) \rangle &= \frac{\pi^2}{2} \delta(\mathbf{k}_1 - \mathbf{k}_2) \delta^{s_1 s_2} \int_0^\infty dv \int_{|1-v|}^{1+v} du \left[\frac{4v^2 - (1 - u^2 + v^2)^2}{4uv} \right]^2 \\ &\times k F(u, v, \bar{\eta}_1) F^*(u, v, \bar{\eta}_2) \mathcal{P}_\phi(vk) \mathcal{P}_\phi(uk). \end{aligned} \quad (3.25)$$

Defining the GW power spectrum by

$$\langle h_{\mathbf{k}_1}^{s_1}(\eta) h_{\mathbf{k}_2}^{s_2,*}(\eta) \rangle \equiv \delta^{(3)}(\mathbf{k}_1 - \mathbf{k}_2) \delta^{s_1 s_2} \frac{2\pi^2}{k^3} \mathcal{P}_h(\eta, k), \quad (3.26)$$

where we have adopted $\mathbf{k}_1 = \mathbf{k}_2 \equiv \mathbf{k}$. Combining with Eqs. (3.18) and (3.25), the power spectrum of the GW is then given by

$$\mathcal{P}_h(\eta, k) = 4 \int_0^\infty dv \int_{|1-v|}^{1+v} du \left[\frac{4v^2 - (1 - u^2 + v^2)^2}{4uv} \right]^2 I^2(u, v, x) \mathcal{P}_\phi(vk) \mathcal{P}_\phi(uk), \quad (3.27)$$

with the kernel function

$$I(u, v, x) = \int_{x_0}^x d\bar{x} \frac{a(\bar{x})}{a(x)} k G_k(x, \bar{x}) F_k(u, v, \bar{x}), \quad (3.28)$$

where we have used $x = k\eta$.

The fraction of the GW energy density per logarithmic wavelength $\Omega_{\text{GW}}(\eta, k)$ is defined by

$$\rho_{\text{GW}}(\eta) \equiv \rho_{\text{tot}}(\eta) \int \Omega_{\text{GW}}(\eta, k) d \ln k, \quad (3.29)$$

where $\rho_{\text{tot}} = 3M_{\text{Pl}}^2 \mathcal{H}^2 / a^2$ is the total energy density of the Universe. With Eq. (3.17) and (3.26), we have

$$\Omega_{\text{GW}}(\eta, k) = \frac{1}{48} \left[\frac{k}{\mathcal{H}(\eta)} \right]^2 \overline{\mathcal{P}_h(\eta, k)} = \frac{1}{48} x^2 \overline{\mathcal{P}_h(\eta, k)}. \quad (3.30)$$

In the second equality, we have used $\mathcal{H} = 1/\eta$ in the radiation-dominated Universe. The spectrum of the GW is directly determined by its power spectrum. In this section, we have calculated the general induced GW from the second-order scalar perturbations. Once the curvature perturbation and its power spectrum are determined, we can calculate the correlator of the source and then determine the power spectrum of the tensor mode.

4 Gravitational wave from perturbation of domain wall

With the results given in section 2 and 3, we can now calculate the second-order tensor power spectrum from the scalar perturbation of the DW network in a radiation-dominated Universe.

4.1 Spectrum before domain wall annihilation

Before the DW annihilation takes place at a conformal time η_a , DWs act as a continuous source for the scalar perturbations whose potential is given by

$$\Phi_k(\eta) = \frac{C f_w(\eta)}{2} \sqrt{\frac{\pi}{2k}} \delta\left(k - \frac{2\pi}{d_w}\right) \quad \text{for } \eta_i \leq \eta \leq \eta_a. \quad (4.1)$$

Using the transfer function in Eq (2.17) and notice that $d(f(x)\delta(x-x_0))/dx = 0$, Eq. (3.9) gives

$$F(u, v, x) = 3T(vx)T(ux) = 3(ux)^5(vx)^5\delta(u-v)\delta(ux-4\pi\mathcal{A}). \quad (4.2)$$

With Eq. (3.28) and the Green's function (3.15) in the radiation-dominated Universe, we then have

$$I_f(u, v, x) = 3\delta(u-v)u^4v^5 \frac{\bar{x}^{11} \sin(x-\bar{x})}{x} \Big|_{\bar{x}=\frac{4\pi\mathcal{A}}{u}}. \quad (4.3)$$

Together with the power spectrum (2.20) of the potential we obtain

$$\mathcal{P}_{h,f}(\eta, k) = \left[\frac{3(4\pi\mathcal{A})^{11} B^2}{\pi^2 k^8 x} \right]^2 \int_{\max(1/2, k_a/k)}^{k_i/k} \left(\frac{4v^2-1}{4v^2} \right)^2 \left[\frac{\sin\left(x - \frac{4\pi\mathcal{A}}{v}\right)}{v^{10}} \right]^2 dv, \quad (4.4)$$

where $k_i = 4\pi\mathcal{A}/\eta_i$ and $k_a = 4\pi\mathcal{A}/\eta_a$ denote the co-moving wavenumber at the time when the DWs form and annihilate, respectively. The condition $v = u > |1-v|$ requires $v > 1/2$ and the momentum should be in the range of $k_a \leq k \leq k_i$. We focus on the GW spectrum at present, i.e., $\eta, x \rightarrow \infty$. Average over the oscillation in the large time limit, the GW spectrum is found to be

$$\Omega_{\text{GW},f}(\eta, k) = \frac{3}{32} \left[\frac{(4\pi\mathcal{A})^{11} B^2}{\pi^2 k^8} \right]^2 \left(-\frac{1}{42s_a^{21}} + \frac{1}{368s_a^{23}} + \frac{1}{19s_a^{19}} - \frac{1}{19s_b^{19}} + \frac{1}{42s_b^{21}} - \frac{1}{368s_b^{23}} \right), \quad (4.5)$$

where we have used $k/\mathcal{H} = k\eta = x$, $s_a = \max(1/2, k_a/k)$, and $s_b = k_i/k$.

4.2 Spectrum after domain wall annihilation

After the annihilation of the DW, the source is removed and the evolution of the curvature perturbation is described by

$$\Phi_k'' + 3\mathcal{H}(1+c_s^2)\Phi_k' + c_s^2 k^2 \Phi_k = 0, \quad (4.6)$$

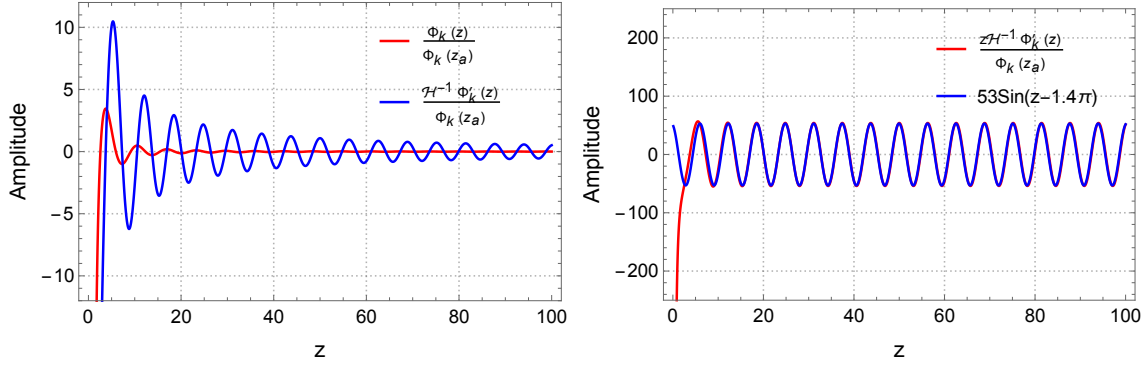


Figure 2: The amplitudes of $\Phi_k(z)$ and $\mathcal{H}^{-1}\Phi'_k(z)$.

where the speed of sound $c_s^2 = \omega$ and the expansion rate $\mathcal{H} = a'/a = 2/((1+3\omega)\eta)$. Eq. (4.6) can be converted into a Bessel equation for $\mathbf{u}_k = \eta\Phi_k$

$$\mathbf{u}_k'' + \mu \frac{\mathbf{u}_k'}{\eta} + \left(\omega k^2 - \frac{\mu}{\eta^2} \right) \mathbf{u}_k = 0 \quad (4.7)$$

where $\mu = \left[\frac{6(1+\omega)}{1+3\omega} - 2 \right]$. For the radiation dominated Universe with $c_s^2 \equiv \omega = 1/3$ and $\mu = 2$, the solution is then given by

$$\Phi_k(\eta) = \frac{1}{z} [C_1(k)j_1(z) + C_2(k)y_1(z)], \quad (4.8)$$

where $z = c_s k \eta$ and $j_n(z)$ and $y_n(z)$ are the spherical Bessel functions of order n . To determine the constants C_1 and C_2 , we require the continuity of Φ_k and Φ'_k (see also [16]) when the DWs annihilate at the time η_a . The derivative of Eq. (4.8) with respect to the conformal time gives

$$\Phi'_k(\eta) = -\frac{c_s k}{z} [C_1(k)j_2(z) + C_2(k)y_2(z)]. \quad (4.9)$$

While we have $\Phi'_k = 0$ for Eq. (4.1) due to the Dirac-delta function. Using the relation $j_1(z)y_2(z) - y_1(z)j_2(z) = -1/z^2$, we have

$$C_1(k) = -z_a^3 y_2(z_a) \Phi_k(\eta_a), \quad \text{and} \quad C_2(k) = z_a^3 j_2(z_a) \Phi_k(\eta_a), \quad (4.10)$$

where $z_a = c_s k \eta_a = 4\pi \mathcal{A} c_s$. Using Eq. (2.17) we then obtain

$$C_1(k) = (4\pi \mathcal{A})^8 c_s^3 y_2(4\pi \mathcal{A} c_s) \frac{B}{k^5 \sqrt{k}}, \quad (4.11)$$

$$C_2(k) = (4\pi \mathcal{A})^8 c_s^3 j_2(4\pi \mathcal{A} c_s) \frac{B}{k^5 \sqrt{k}}. \quad (4.12)$$

For $\mathcal{A} = 1$ and $\omega = 1/3$, we have $j_2(z_a) = -0.139$ and $y_2(z_a) = 0.026$, then we obtain $C_1 = -10\Phi_k(\eta_a)$ and $C_2 = -53\Phi_k(\eta_a)$.

In the left panel of Fig. 2, we plot $\Phi_k(z)/\Phi_k(\eta_a)$ and $\mathcal{H}^{-1}\Phi'_k(z)/\Phi_k(\eta_a)$ as a function of z . We therefore observe that compared with $\mathcal{H}^{-1}\Phi'_k(z)$, $\Phi_k(z)$ is negligible for the source term (3.7). From the right panel of Fig. 2, we show that $\mathcal{H}^{-1}\Phi'_k(z)$ can be approximated by a sine function as $z \rightarrow \infty$, i.e.,

$$\mathcal{H}^{-1}\Phi'_k(z) \simeq -\frac{C_2(k)}{z} \sin(z - \theta_a), \quad (4.13)$$

where $\theta_a = 1.4\pi$. The exact value of θ_a is trivial for us. This indicates the term with coefficient C_2 is the dominant component for the conformal time derivative of the potential. The source term (3.7) then can be written as

$$S_{\mathbf{k}}^s(\eta) \simeq \int \frac{d^3\mathbf{q}}{(2\pi)^{3/2}} e^{s(\mathbf{k}, \mathbf{q})} \frac{C_2(vk)C_2(uk)}{uvz^2} \sin(vz - \theta_a) \sin(uz - \theta_a). \quad (4.14)$$

Comparing with Eq. (3.8) and the definition of the power spectrum (2.19), we have

$$F(u, v, z) = \frac{1}{uvz^2} \sin(vz - \theta_a) \sin(uz - \theta_a) \quad \text{and} \quad \mathcal{P}(k) = \frac{k^3 C_2^2(k)}{2\pi^2}, \quad (4.15)$$

and

$$I(u, v, x) = \int_{x_a}^x d\bar{x} \frac{\bar{x}}{x} \sin(x - \bar{x}) \frac{1}{uv\bar{z}^2} \sin(v\bar{z} - \theta_a) \sin(u\bar{z} - \theta_a). \quad (4.16)$$

The integration for Eq. (4.16) can be solved analytically with the following relations

$$\begin{aligned} & \int_{x_a}^x d\bar{x} \frac{1}{\bar{x}} \sin(x - \bar{x}) \sin(a\bar{x} - \theta_a) \sin(b\bar{x} - \theta_a) = \\ & \frac{1}{4} \{ -\text{Ci}((a+b+1)x) \sin(2\theta_a + x) - \text{Ci}((a+b-1)x) \sin(x - 2\theta_a) + \text{Ci}((a+b+1)x_a) \sin(2\theta_a + x) \\ & + \text{Ci}((a+b-1)x_a) \sin(x - 2\theta_a) - \sin(x) \text{Ci}((a-b-1)x_a) - \sin(x) \text{Ci}((a-b+1)x_a) \\ & + \sin(x) \text{Ci}((a-b-1)x) + \sin(x) \text{Ci}((a-b+1)x) - \text{Si}((a+b-1)x) \cos(x - 2\theta_a) \\ & + \text{Si}((a+b+1)x) \cos(2\theta_a + x) + \text{Si}((a+b-1)x_a) \cos(x - 2\theta_a) - \text{Si}((a+b+1)x_a) \cos(2\theta_a + x) \\ & - \cos(x) \text{Si}((a-b-1)x_a) + \cos(x) \text{Si}((a-b+1)x_a) + \cos(x) \text{Si}((a-b-1)x) - \cos(x) \text{Si}((a-b+1)x) \}, \end{aligned} \quad (4.17)$$

where $a = c_s v$ and $b = c_s u$. $\text{Ci}(x) \equiv -\int_x^\infty dy \cos(y)/y$ and $\text{Si}(x) \equiv \int_0^x dy \sin(y)/y$ are the cosine and sine integrals, respectively.

The results of Eq. (4.17) can be approximated by two significant contributions [15]. One of them is the case $\text{Ci}(0) \rightarrow -\infty$ and $\text{Si}(0) = 0$, which corresponds to the resonant production of GW. The limits $|1-v| < u < 1+v$ and $u > 0$ and $v > 0$ give $u+v > 1$ and $u-v < 1$. Therefore the resonant production of GWs can take place when $u+v = 1/c_s = \sqrt{3}$. Then the corresponding kernel function for the resonant production is given by

$$I_{\text{res}}(u, v, x) = \frac{\sin(x - 2\theta_a)}{4\omega uvx} \{ \text{Ci}[(c_s v + c_s u - 1)x_a] - \text{Ci}[(c_s v + c_s u - 1)x] \}, \quad \text{with } u+v = 1/c_s. \quad (4.18)$$

The other significant contribution comes from the large $u \simeq v \gg 1$ limit, corresponding to the situation $\text{Si}(\infty) = \pi/2$ and $\text{Ci}(\infty) = 0$. For the late time $x \rightarrow \infty$, the kernel function in the large v limit is given by

$$I_{\text{LV}}(u, v, x) = \frac{1}{4\omega uvx} \left[-\sin x \text{Ci}(x_a) + \cos x \left(\text{Si}(x_a) - \frac{\pi}{2} \right) \right] \quad \text{with } u = v \gg 1. \quad (4.19)$$

Then the squared kernel functions averaged over the late time limit $x \rightarrow \infty$ are given by [15, 16]

$$\overline{I_{\text{res}}^2(u = c_s^{-1} - v, v, x_a)} \simeq \frac{1}{32\omega^2 u^2 v^2 x^2} \text{Ci}^2[(c_s v + c_s u - 1)x_a] \quad (4.20)$$

and

$$\overline{I_{\text{LV}}^2(u = v, v, x)} \simeq \frac{1}{32\omega^2 u^2 v^2 x^2} \left[\text{Ci}^2(x_a) + \left(\text{Si}(x_a) - \frac{\pi}{2} \right)^2 \right]. \quad (4.21)$$

We now consider the GW spectrum from the perturbations after the annihilation of the wall. According to different evolution stages of the DW, the kernel function for the perturbation can be split into two parts

$$I(u, v, x) = I_f(u, v, x, x_i, x_a) + I_a(u, v, x, x_a), \quad (4.22)$$

where I_f denotes the kernel function between the formation and annihilation of the DW and I_a denotes the kernel function after the annihilation of the wall. We can neglect the cross term $\overline{I_f I_a}$ in $\overline{I^2}$ since the time average of the oscillation in the squared kernel function could lead to a strong suppression of the cross term [16]. The energy density of the GW is then given by

$$\begin{aligned} \Omega_{\text{GW}}(\eta, k) &= \frac{1}{48} \left(\frac{k}{\mathcal{H}} \right)^2 \overline{\mathcal{P}_h(\eta, k)} \simeq \frac{1}{48} \left(\frac{k}{\mathcal{H}} \right)^2 \left(\overline{\mathcal{P}_{h,f}(\eta, k)} + \overline{\mathcal{P}_{h,a}(\eta, k)} \right) \\ &\equiv \Omega_{\text{GW},f}(\eta, k) + \Omega_{\text{GW},a}(\eta, k), \end{aligned} \quad (4.23)$$

with $\Omega_{\text{GW},f}(\eta, k)$ given by Eq. (4.5). Since the resonant production and large v contributions take place in two different parameter regimes, the power spectrum of the perturbation after the DW annihilation $\overline{\mathcal{P}_{h,a}(\eta, k)}$ can be approximated as

$$\overline{\mathcal{P}_{h,a}(\eta, k)} \simeq \overline{\mathcal{P}_{h,a,\text{res}}(\eta, k)} + \overline{\mathcal{P}_{h,a,\text{LV}}(\eta, k)}. \quad (4.24)$$

Let us first calculate the resonant production of the GW, which is significant at the parameter regime $u + v \simeq c_s^{-1}$. With Eqs. (3.27), (4.15) and (4.20) we have

$$\begin{aligned} \overline{\mathcal{P}_{h,a,\text{res}}(\eta, k)} &= \frac{1}{8\omega^2 x^2} \int_{k_a/k}^{k_i/k} dv \int_{\max(|1-v|, k_a/k)}^{\min(1+v, k_i/k)} du \left[\frac{4v^2 - (1 - u^2 + v^2)^2}{4u^2 v^2} \right]^2 \\ &\quad \times \frac{v^3 k^3 C_2^2(vk)}{2\pi^2} \frac{u^3 k^3 C_2^2(uk)}{2\pi^2} \text{Ci}^2[(c_s v + c_s u - 1)x_a]. \end{aligned} \quad (4.25)$$

To perform the integration, we change the integration variables to $t = (c_s v + c_s u - 1)x_a$ and $s = u - v$ with a Jacobian factor $1/(2c_s x_a)$. The resonant contribution comes from

the integration at point $t = 0$. We, therefore, set $t = 0$ for the integrant except for Ci function [15, 16], which has a spiky value at this point. Integating Ci gives a factor $\simeq \pi$, i.e., $\int_{-\infty}^{\infty} dt \text{Ci}^2(|t|) = \pi$. With these approximations, the integration is simplified as

$$\overline{\mathcal{P}_{h,a,\text{res}}(\eta, k)} = \frac{4^5 \omega^6 (1 - \omega)^2 \widehat{C}_2^4}{\pi^3 c_s x_a x^2 k^{16}} \int_{s_1(k)}^{s_2(k)} ds \frac{(1 - s^2)^2}{(1 - \omega s^2)^{10}}, \quad (4.26)$$

where $\widehat{C}_2 = (4\pi\mathcal{A})^8 c_s^3 j_2(4\pi\mathcal{A}c_s)B$. The condition $u > |1 - v|$ gives $u > (c_s^{-1} - 1)/2$ (assuming $c_s^{-1} > 1$), which restricts the lower limit of the integration in the range of $-1 \leq s_1(k) \leq 0$. With the relation $s = 2u - c_s^{-1}$, we have $u = c_s^{-1}/2$ for $s_1(k) = 0$ and $u = (c_s^{-1} - 1)/2$ for $s_1(k) = -1$. Taking into account the limit $u \geq u_{\min} = k_a/k$ we have

$$s_1(k) = \begin{cases} -1 & \frac{k_a}{k} < \frac{c_s^{-1} - 1}{2}, \\ 2\frac{k_a}{k} - c_s^{-1} & \frac{c_s^{-1} - 1}{2} \leq \frac{k_a}{k} \leq \frac{c_s^{-1}}{2}, \\ 0 & \frac{k_a}{k} > \frac{c_s^{-1}}{2}. \end{cases} \quad (4.27)$$

Again, the condition $u < 1 + v$ restricts the upper limit of the integration in the range of $0 \leq s_0(k) \leq 1$. We then have $u = c_s^{-1}/2$ for $s_2(k) = 0$ and $u = (1 + c_s^{-1})/2$ for $s_2(k) = 1$. Taking into account the limit $u \leq u_{\max} = k_i/k$ we obtain

$$s_2(k) = \begin{cases} 1 & \frac{k_i}{k} > \frac{1 + c_s^{-1}}{2}, \\ 2\frac{k_i}{k} - c_s^{-1} & \frac{c_s^{-1}}{2} \leq \frac{k_i}{k} \leq \frac{1 + c_s^{-1}}{2}, \\ 0 & \frac{k_i}{k} < \frac{c_s^{-1}}{2}. \end{cases} \quad (4.28)$$

With $|s_{1(2)}| \sim 1$, the result of the integration is ~ 2 . We can also convert the integration variable s back to u with the relation $s = 2u - c_s^{-1}$, then the resonant contribution to the GW spectrum is found to be

$$\Omega_{\text{GW},a,\text{res}}(\eta, k) = \frac{4^5 \omega^6 (1 - \omega)^2 \widehat{C}_2^4}{48\pi^3 c_s x_a k^{16}} \int_{u_a(k)}^{u_b(k)} du \frac{2[1 - (2u - c_s^{-1})^2]^2}{[1 - \omega(2u - c_s^{-1})^2]^{10}}, \quad (4.29)$$

where $u_a(k) = \max((c_s^{-1} - 1)/2, k_a/k)$ and $u_b(k) = \min((c_s^{-1} + 1)/2, k_i/k)$. The integration has an analytical expression, which is tedious and is not shown here.

With the squared kernel function (4.21), the power spectrum from large v contributions is given by

$$\begin{aligned} \overline{\mathcal{P}_{h,a,\text{LV}}(\eta, k)} &= \frac{1}{8\omega^2 x^2} \int_{\max(1/2, k_a/k)}^{k_i/k} dv \int_{\max(|1-v|, k_a/k)}^{\min(1+v, k_i/k)} du \left[\frac{4v^2 - (1 - u^2 + v^2)^2}{4u^2 v^2} \right]^2 \\ &\times \frac{v^3 k^3 C_2^2(vk)}{2\pi^2} \frac{u^3 k^3 C_2^2(uk)}{2\pi^2} \left[\text{Ci}^2(x_a) + \left(\text{Si}(x_a) - \frac{\pi}{2} \right)^2 \right]. \end{aligned} \quad (4.30)$$

For the large v contribution, we can set $u \simeq v \gg 1$. Therefore, we can insert $\delta(u - v)$ into Eq. (4.30) and the GW spectrum is found to be

$$\Omega_{\text{GW},a,\text{LV}}(\eta, k) = \frac{\hat{C}_2^4}{1536\pi^4\omega^2k^{16}} \left[\text{Ci}^2(x_a) + \left(\text{Si}(x_a) - \frac{\pi}{2} \right)^2 \right] \times \left(-\frac{1}{42s_a^{21}} + \frac{1}{368s_a^{23}} + \frac{1}{19s_a^{19}} - \frac{1}{19s_b^{19}} + \frac{1}{42s_b^{21}} - \frac{1}{368s_b^{23}} \right), \quad (4.31)$$

where $s_a = \max(1/2, k_a/k)$ and $s_b = k_i/k$. We observe that the k -dependence in Eq. (4.31) is the same as that in Eq. (4.5), thus, the GW spectra of both are the same except for the amplitudes. This is because both spectra are derived under the condition $u = v$.

4.3 Results

Our main results are represented by the GW spectrum given by Eqs. (4.5), (4.29), and (4.31). The total GW spectrum induced by the DW perturbations is then given by the sum of these contributions

$$\Omega_{\text{GW,tot}} = \Omega_{\text{GW},f} + \Omega_{\text{GW},a,\text{res}} + \Omega_{\text{GW},a,\text{LV}}. \quad (4.32)$$

We show these results in Fig. 3. In this plot, we have assumed the DW generated at a cosmic temperature $T = 10^8$ GeV and annihilates at $T = 10^4$ GeV, which correspond to the frequencies $k_i = 1492.3$ Hz and $k_a = 0.15$ Hz of the scalar perturbation at formation and annihilation. During this period, DWs do not dominate the Universe.

From Fig. 3 we observe that the shape of the GW spectrum from the DW before annihilation (represented by the orange dotted line) is the same as that from large v contribution after DW annihilation (green dashed line). But the amplitude of the former is much smaller than the latter, and therefore, is negligible. The resonant productions of GWs (blue dot-dashed line) take place when the GW frequency equals the frequency of the perturbation at annihilation, i.e., $k \simeq k_a$. For $k \lesssim k_a$, the large v contribution dominates the spectrum. We see that the spectrum from resonant production peaks at $k \simeq k_a$, which enhances the GW signal by about four orders of magnitude. Note that the scalar perturbations from DW are horizon-sized. Therefore, the oscillation modes of the GWs are superhorizon if their frequencies are lower than that of the perturbation during the annihilation of the wall, i.e., $k \lesssim k_a$. Then the causality requires the superhorizon modes scale as k^3 , as shown in Fig. 3. For high frequencies $k \gtrsim k_a$, the modes are inside the horizon and the GWs decay away as k^{-16} .

Finally, the example we show in Fig. 3 has a peak amplitude of the induced GW signal at $\Omega_{\text{GW}} \sim 10^{-22}$, which is beyond the sensitivities of current and near-future GW experiments. The power spectrum of the curvature perturbation of the DW is proportional to k^{-8} , therefore, the GW signals could be largely enhanced and enter into the detection zone of the experiments if the annihilation of DW takes place much later.

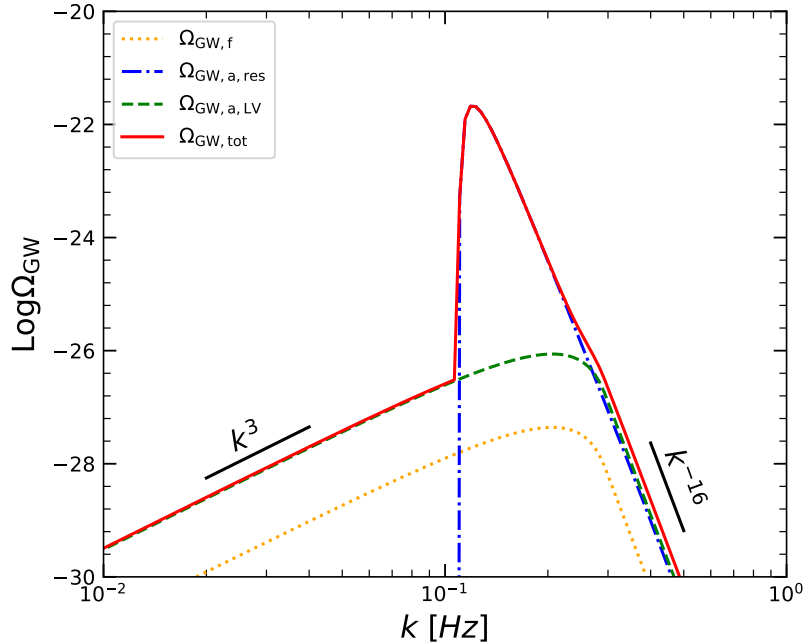


Figure 3: The induced GW spectrum Ω_{GW} from DW scalar perturbations as a function of the frequency today.

5 Conclusions

The DW is an important topological defect that formed during the spontaneous breaking of a discrete symmetry. The discrete symmetries commonly exist in various new particle physics, and therefore, the detection of the gravitational wave spectrum from the DW evolution can be a unique approach to testing the physics beyond the standard model. The GWs from the annihilation of the DW have been widely considered in previous literature. In this work, we provide for the first time the scalar-induced GW spectrum from the perturbations of the wall. We find that the spectrum has a sharp peak at frequency $k \simeq k_a$ (where k_a is the frequency of the perturbation during the annihilation of the DW), which largely enhances the signal to be detectable for the experiments. For subhorizon modes with $k \gtrsim k_a$, the spectrum decays as $\propto k^{-16}$. While for the superhorizon modes with $k \lesssim k_a$, the spectrum scales as $\propto k^3$, which is consistent with the causality. The induced GW signals from DW perturbations are distinguishable from the other GW sources, such as first-order phase transition, inflation, and cosmic string. The detection of this signal in various GW experiments, including PTAs, LISA, Taiji, Tianqin, and LIGO, will be presented in the upcoming work.

Acknowledgements

BQL is supported in part by the National Natural Science Foundation of China under Grant No. 12405058 and by the Zhejiang Provincial Natural Science Foundation of China under Grant No. LQ23A050002.

A Domain wall evolution

With the one-scale assumption $\rho_w = \sigma_w/L_w$, the evolution of the DW is described by the following equations

$$\begin{aligned}\frac{dL_w}{dt} &= HL_w + \frac{L_w}{\ell_d} v_w^2 + c_w v_w, \\ \frac{dv_w}{dt} &= (1 - v_w^2) \left(\frac{k_w}{L_w} - \frac{v_w}{\ell_d} \right),\end{aligned}\tag{A.1}$$

where v_w is the averaged velocity of the wall and the chopping parameter $c_w = 0.81 \pm 0.04$ from the simulations of the domain wall evolution in the Z_2 model [33]. The damping length is defined as

$$\frac{1}{\ell_d} = 3H + \frac{1}{\ell_f},\tag{A.2}$$

which includes the damping effects on the network from Hubble drag and particle friction, which is related to the particle pressure ΔP by

$$\frac{1}{\ell_f} = \frac{\Delta P}{v_w \sigma_w}.\tag{A.3}$$

In usual models the particle friction is negligible.

References

- [1] **LIGO Scientific, Virgo** Collaboration, B. P. Abbott et al., *Observation of Gravitational Waves from a Binary Black Hole Merger*, Phys. Rev. Lett. **116** (2016), no. 6 061102, [[1602.03837](#)].
- [2] **NANOGrav** Collaboration, G. Agazie et al., *The NANOGrav 15 yr Data Set: Evidence for a Gravitational-wave Background*, Astrophys. J. Lett. **951** (2023), no. 1 L8, [[2306.16213](#)].
- [3] **EPTA** Collaboration, J. Antoniadis et al., *The second data release from the European Pulsar Timing Array III. Search for gravitational wave signals*, [2306.16214](#).
- [4] D. J. Reardon et al., *Search for an Isotropic Gravitational-wave Background with the Parkes Pulsar Timing Array*, Astrophys. J. Lett. **951** (2023), no. 1 L6, [[2306.16215](#)].
- [5] H. Xu et al., *Searching for the Nano-Hertz Stochastic Gravitational Wave Background with the Chinese Pulsar Timing Array Data Release I*, Res. Astron. Astrophys. **23** (2023), no. 7 075024, [[2306.16216](#)].
- [6] C. Caprini and D. G. Figueroa, *Cosmological Backgrounds of Gravitational Waves*, Class. Quant. Grav. **35** (2018), no. 16 163001, [[1801.04268](#)].

- [7] G. Domènech, *Scalar Induced Gravitational Waves Review*, Universe **7** (2021), no. 11 398, [[2109.01398](#)].
- [8] K. N. Ananda, C. Clarkson, and D. Wands, *The Cosmological gravitational wave background from primordial density perturbations*, Phys. Rev. D **75** (2007) 123518, [[gr-qc/0612013](#)].
- [9] E. Bugaev and P. Klimai, *Induced gravitational wave background and primordial black holes*, Phys. Rev. D **81** (2010) 023517, [[0908.0664](#)].
- [10] L. Alabidi, K. Kohri, M. Sasaki, and Y. Sendouda, *Observable Spectra of Induced Gravitational Waves from Inflation*, JCAP **09** (2012) 017, [[1203.4663](#)].
- [11] H. Assadullahi and D. Wands, *Gravitational waves from an early matter era*, Phys. Rev. D **79** (2009) 083511, [[0901.0989](#)].
- [12] L. Alabidi, K. Kohri, M. Sasaki, and Y. Sendouda, *Observable induced gravitational waves from an early matter phase*, JCAP **05** (2013) 033, [[1303.4519](#)].
- [13] E. D. Kovetz, *Probing Primordial-Black-Hole Dark Matter with Gravitational Waves*, Phys. Rev. Lett. **119** (2017), no. 13 131301, [[1705.09182](#)].
- [14] K. Kohri and T. Terada, *Semianalytic calculation of gravitational wave spectrum nonlinearly induced from primordial curvature perturbations*, Phys. Rev. D **97** (2018), no. 12 123532, [[1804.08577](#)].
- [15] K. Inomata, K. Kohri, T. Nakama, and T. Terada, *Enhancement of Gravitational Waves Induced by Scalar Perturbations due to a Sudden Transition from an Early Matter Era to the Radiation Era*, Phys. Rev. D **100** (2019) 043532, [[1904.12879](#)]. [Erratum: Phys.Rev.D 108, 049901 (2023)].
- [16] G. Domènech, C. Lin, and M. Sasaki, *Gravitational wave constraints on the primordial black hole dominated early universe*, JCAP **04** (2021) 062, [[2012.08151](#)]. [Erratum: JCAP 11, E01 (2021)].
- [17] C.-W. Chiang and B.-Q. Lu, *Testing clockwork axion with gravitational waves*, JCAP **05** (2021) 049, [[2012.14071](#)].
- [18] B.-Q. Lu, C.-W. Chiang, and T. Li, *Clockwork axion footprint on nanohertz stochastic gravitational wave background*, Phys. Rev. D **109** (2024), no. 10 L101304, [[2307.00746](#)].
- [19] J. Antoniadis et al., *The International Pulsar Timing Array second data release: Search for an isotropic gravitational wave background*, Mon. Not. Roy. Astron. Soc. **510** (2022), no. 4 4873–4887, [[2201.03980](#)].
- [20] B.-Q. Lu, C.-W. Chiang, and T. Li, *Primordial black hole from domain wall fluctuations*, [2409.09986](#).
- [21] B.-Q. Lu, C.-W. Chiang, and T. Li, *A Common Origin for Nano-Hz Gravitational Wave Background and Black Hole Merger Events*, [2409.10251](#).
- [22] R. Saito and J. Yokoyama, *Gravitational wave background as a probe of the primordial black hole abundance*, Phys. Rev. Lett. **102** (2009) 161101, [[0812.4339](#)]. [Erratum: Phys.Rev.Lett. 107, 069901 (2011)].
- [23] R. Saito and J. Yokoyama, *Gravitational-Wave Constraints on the Abundance of Primordial*

- Black Holes*, Prog. Theor. Phys. **123** (2010) 867–886, [[0912.5317](#)]. [Erratum: Prog.Theor.Phys. 126, 351–352 (2011)].
- [24] V. De Luca, G. Franciolini, A. Kehagias, and A. Riotto, *On the Gauge Invariance of Cosmological Gravitational Waves*, JCAP **03** (2020) 014, [[1911.09689](#)].
- [25] K. Inomata and T. Terada, *Gauge Independence of Induced Gravitational Waves*, Phys. Rev. D **101** (2020), no. 2 023523, [[1912.00785](#)].
- [26] C. Yuan, Z.-C. Chen, and Q.-G. Huang, *Scalar induced gravitational waves in different gauges*, Phys. Rev. D **101** (2020), no. 6 063018, [[1912.00885](#)].
- [27] A. Vilenkin, *Cosmic Strings and Domain Walls*, Phys. Rept. **121** (1985) 263–315.
- [28] Y. Nambu, H. Ishihara, N. Gouda, and N. Sugiyama, *Anisotropies of the cosmic background radiation by domain wall networks*, .
- [29] N. Kaiser and J. A. Peacock, *Power spectrum analysis of one-dimensional redshift surveys*, Astrophys. J. **379** (1991) 482–506.
- [30] T. Hiramatsu, M. Kawasaki, and K. Saikawa, *On the estimation of gravitational wave spectrum from cosmic domain walls*, JCAP **02** (2014) 031, [[1309.5001](#)].
- [31] D. Baumann, P. J. Steinhardt, K. Takahashi, and K. Ichiki, *Gravitational Wave Spectrum Induced by Primordial Scalar Perturbations*, Phys. Rev. D **76** (2007) 084019, [[hep-th/0703290](#)].
- [32] T. Papanikolaou, V. Vennin, and D. Langlois, *Gravitational waves from a universe filled with primordial black holes*, JCAP **03** (2021) 053, [[2010.11573](#)].
- [33] C. J. A. P. Martins, I. Y. Rybak, A. Avgoustidis, and E. P. S. Shellard, *Extending the velocity-dependent one-scale model for domain walls*, Phys. Rev. D **93** (2016), no. 4 043534, [[1602.01322](#)].